Analytical Approach for Optimal Deployment of Drone Base Stations in Cellular Networks

Pijnappel, T.R.; van den Berg, J.L.; Borst, S.C.; Litjens, R.

DOI
10.1109/ICC45041.2023.10278620

Publication date
2023

Document Version
Final published version

Published in
Proceedings of the ICC 2023 - IEEE International Conference on Communications

Analytical Approach for Optimal Deployment of Drone Base Stations in Cellular Networks

T.R. Pijnappel*, J.L. van den Berg†, S.C. Borst*, R. Litjens§‡

*Eindhoven University of Technology, Eindhoven, The Netherlands
†University of Twente, Enschede, The Netherlands
§TNO, The Hague, The Netherlands
‡Delft University of Technology, Delft, The Netherlands

***Abstract*—Reliable mobile communications is of critical importance, and should be maintained even in case of extremely crowded events or emergency scenarios. In such scenarios the deployment of drone-mounted base stations offers an agile and cost-efficient way to sustain coverage and/or provide capacity relief. In this paper we develop an analytical method to estimate the blocking and coverage probabilities of drone-assisted cellular networks using information that is readily available from network planning tools. We demonstrate how this method can be used to determine the minimum required number of drones and their corresponding locations for a given target performance level.**

***Index Terms*—Beyond 5G, drone base station positioning, call success rate, multi-class loss systems**

I. Introduction

In case of unanticipated incidents, such as network disruptions (due to disasters such as earthquakes or floodings) or crowded events, the quality of service in wireless cellular networks may be severely degraded. In such situations, it is of utmost importance to swiftly add capacity and/or restore coverage of the network. An agile and cost-efficient way to achieve this in beyond 5G networks is by deploying drone-mounted base stations [1]. Effective deployment of drone base stations involves optimization of the number of deployed drones and their associated (initial) control parameters (e.g., locations and cell selection biases).

In view of the goal to improve capacity and/or coverage, a natural optimization objective is to maximize the Call Success Rate (CSR), minimize the fraction of blocked users or minimize the number of users that do not have coverage. However, these performance metrics are strongly influenced by the number of deployed drones and their control parameters. Moreover, in an online setting (where the control parameters are adjusted based on real-time measurements), it takes a long time to accurately measure the CSR. This implies that adaptive optimization based on the CSR can be prohibitively slow when the initial set of control parameters has poor performance, which is especially undesirable in emergency scenarios. Thus a good initial set of control parameters provides crucial benefits for the online optimization and the CSR performance.

In this paper we propose and demonstrate an iterative method to find a suitable set of control parameters in an offline setting. Specifically, the method relies on an analytic model consisting of several coupled multi-class loss systems, where the different classes reflect the heterogeneous resource requirements of the users. Furthermore, the parameters of these loss systems are functions of the number of drones and associated control parameters. These functions in turn depend on the ambient network parameters and environmental characteristics (e.g., the spatial traffic distribution and the propagation environment), which can be extracted from a network planning tool. Given the environmental characteristics and the control parameters of the drones, the model provides estimates for the CSR and blocking and coverage probabilities.

The proposed method is suitable for offline optimization since it only requires information that can be obtained from a planning tool. In particular, the method can be used to determine the number of drones needed to achieve a desired CSR level, along with the corresponding set of control parameters. This obtained set of control parameters can then be further tuned and dynamically adjusted using real-time measurements, which dovetails with the online algorithm for drone positioning proposed in [2].

A. Related literature

Optimization of the number and positioning of drone base stations has been studied in several papers. In [3] the authors consider a method for the deployment of drone base stations based on the notion of truncated octahedron shapes, which ensures full coverage for a given space with a minimum number of drones. In this method, the number of drones is equal to the number of truncated octahedron cells needed to cover a 3D space. In [4], the authors use simulated annealing and a genetic algorithm to find the minimum number of drones and their locations such that the selected area is fully covered with least cost while also considering data rates, latency and throughput. Another paper [5] considers the deployment of various numbers of drones and demonstrates that the proposed mobility control algorithm reduces the number of required drones, while optimizing the spectral efficiency. In [6] the authors formulate a joint optimization problem with the goal to maximize the number of served users with a minimum number of drones and propose a low-complexity heuristic for this. In [7] a method based on particle swarm optimization is proposed to find the minimum required number of drones and their positions such that all users are served. In [8] the authors

ICC 2023 - IEEE International Conference on Communications | 978-1-5386-7462-8/23/$31.00 ©2023 IEEE | DOI: 10.1109/ICC45041.2023.10278620

formulate the drone deployment as a minimization problem subject to coverage constraints. Furthermore, an improved genetic algorithm is proposed for static user scenarios, and a modified version for dynamic user scenarios. In [9] the authors propose an artificial bee colony algorithm for the positioning of drone base stations, and evaluate the performance for various numbers of drones.

As opposed to [3]–[9], we consider a cellular network that consists of both drones and regular sites. Moreover, the method that we propose only relies on the spatial user distribution and propagation characteristics, and does not depend on particular realizations of the user locations. In fact, the method that we propose is more analytic in nature and does not require many or long simulation runs to obtain accurate results.

B. Contributions

The main contributions of this paper are the following: 1) we provide a method to estimate the CSR, blocking and coverage of drone-assisted wireless cellular networks; 2) we demonstrate how the method can be used to determine the required number of drones and their locations to achieve a target CSR level. The found number of drones and associated control parameters in turn provide a good initial set of control parameters for the drone base stations in case of site failures or crowded events.

C. Organization of the paper

In Section II we describe a model that can be used to estimate the blocking and coverage probabilities and CSR. Section III explains how the parameters of the model depend on the propagation environment, spatial user distribution and control parameters, and how these can be calculated. In Section IV we determine the number of classes that the proposed model needs to provide accurate results. Furthermore, we demonstrate for some illustrative scenarios that the proposed model can be used to iteratively find suitable locations for a given number of drone base stations. Section V summarizes the results of this paper and suggests some topics for further research.

II. Performance evaluation model

In order for a call to be successful, it must have coverage and sufficient resources need to be available to accept it. In our method we first determine the arrival rates of calls that have coverage, and then use these as input parameters for a multi-class loss model. Specifically, we consider each of the N_r regular cells and N_d drone cells to be a multi-class loss system. Thus the drone-assisted cellular network will be modeled as $N = N_r + N_d$ coupled multi-class loss systems denoted by $\mathcal{N} = \{1, 2, \ldots, N\}$.

For each loss system we consider C different user classes denoted by $\mathcal{C} = \{1, 2, \ldots, C\}$, where each user class corresponds to users having a resource requirement within a specific range. Moreover, the model parameters of these loss systems depend on the scenario characteristics (traffic intensity, path loss, antenna gain and shadow fading) and the number of drones and associated control parameters (drone locations and cell selection biases, which can be used to steer traffic towards or away from a cell). Specifically, let $\boldsymbol{\lambda} = (\lambda_{i,k}, i \in \mathcal{N}, k \in \mathcal{C})$ and $\boldsymbol{\beta} = (\beta_{i,k}, i \in \mathcal{N}, k \in \mathcal{C})$, where $\lambda_{i,k}$ and $\beta_{i,k}$ denote the Poisson arrival rates, and mean service times of the various user classes at the different loss systems (note that this refers to users that have coverage). Furthermore, let $\boldsymbol{\omega} = (\omega_{i,k}, i \in \mathcal{N}, k \in \mathcal{C})$, with $\omega_{i,k}$ the fraction of resources required by a class-k user at system i.

As mentioned before, the model parameters of the loss systems are functions of the number of drones and associated control parameters. These functions in turn depend on the system model (i.e., propagation characteristics, the locations of the regular sites and their antenna features, etc. which will be described in Section III-A), and we show how $\boldsymbol{\lambda}$, $\boldsymbol{\beta}$ and $\boldsymbol{\omega}$ can be calculated in Section III-B.

Let us now explain how for given model parameters $\boldsymbol{\lambda}$, $\boldsymbol{\beta}$ and $\boldsymbol{\omega}$, the multi-class loss systems can be used to estimate the fraction of blocked calls. First we identify the state space $\mathcal{S}_i$ for each loss system $i \in \mathcal{N}$, namely

$$\mathcal{S}_i = \left\{ \boldsymbol{n} = (n_1, n_2, \ldots, n_C) \in \mathbb{N}^C \;\middle|\; \sum_{k \in \mathcal{C}} n_k \omega_{i,k} \leq 1 \right\},$$

where $\mathbb{N} = \{0, 1, 2, 3, \ldots\}$. Second, we calculate the steady-state distribution $\boldsymbol{\pi}_i$ of system i, i.e., the long-term average probability that system i resides in each state of $\mathcal{S}_i$ using the standard formula for multi-class loss systems [10]

$$\pi_{i,\boldsymbol{n}} = \frac{1}{G_i} \prod_{k \in \mathcal{C}} \frac{(\lambda_{i,k}\beta_{i,k})^{n_k}}{n_k!}, \quad \boldsymbol{n} \in \mathcal{S}_i,$$

with G_i the normalization constant. Third, using the PASTA (Poisson arrivals see time averages) property, the probability that a class-k user at system i will be blocked is given by

$$p_{\text{blocking},i,k} = \sum_{\substack{\boldsymbol{n} \in \mathcal{S}_i, \\ \boldsymbol{n} + \boldsymbol{e}_k \notin \mathcal{S}_i}} \pi_{i,\boldsymbol{n}},$$

where $\boldsymbol{e}_k$ is the k-th unit vector of length C.

Then we can also calculate the overall fraction of users that have coverage but will be blocked, as

$$p_{\text{blocking}} = \sum_{i \in \mathcal{N}} \sum_{k \in \mathcal{C}} \frac{\lambda_{i,k}}{\lambda_{\text{coverage}}} p_{\text{blocking},i,k}.$$

with

$$\lambda_{\text{coverage}} = \sum_{i \in \mathcal{N}} \sum_{k \in \mathcal{C}} \lambda_{i,k}$$

representing the total arrival rate of users that have coverage.

Denote by $\Lambda \geq \lambda_{\text{coverage}}$ the total arrival rate of users (including ones without coverage as will be specified later). The fraction of users that are in outage (and thus not even assigned to one of the loss systems) is

$$p_{\text{outage}} = 1 - \frac{\lambda_{\text{coverage}}}{\Lambda}.$$

The CSR can then be calculated as

$$\begin{aligned}\text{CSR} &= (1 - p_{\text{outage}})(1 - p_{\text{blocking}}) \\ &= \frac{1}{\Lambda} \sum_{i \in \mathcal{N}} \sum_{k \in \mathcal{C}} \lambda_{i,k} \left(1 - p_{\text{blocking},i,k}\right).\end{aligned}$$

III. Derivation of model parameters

In Section III-A we first describe the system model (i.e., the propagation characteristics, spatial user density, base station features, etc.). These modeling assumptions are similar to [2]. Then in Section III-B we show how the system model impacts the functions that determine the parameters ($\boldsymbol{\lambda}$, $\boldsymbol{\beta}$ and $\boldsymbol{\omega}$) of the performance evaluation model.

A. Characterization of system model

For the cellular network, we consider a hexagonal layout of twelve three-sectorized sites with an inter-site distance (ISD) corresponding to a dense urban or rural scenario. Together these sites comprise $N_r = 12 \times 3 = 36$ cells. Besides the regular cells we also have N_d drone cells. Each of the cells in this network is assigned a $B = 5$ MHz carrier in the 3.5 GHz band, where we assume that a fraction $\kappa = 0.25$ of the bandwidth is consumed by control signaling.

Each *regular* cell is equipped with a directional antenna at height h_{antenna}, with a θ_{tilt}-degree downtilt. To determine the antenna gains corresponding to these regular cells, we use the model from [11] with parameters from [12], with a total transmit power of 20 W for each regular cell.

For the *drone* cells, we assume that each drone is equipped with a simple antenna for which we use a rotated version of the model provided in [13, Table 7.3-1], with an adapted vertical component to ensure a circular footprint, and a total transmit power of 0.5 W for each drone cell.

To determine the path loss between a regular cell and a user, we use the path loss models provided in [13, Tables 7.4.1 and 7.4.2] and calculate the path loss as the weighted average of the path loss for a line-of-sight (LoS) and a non line-of-sight (NLoS) link, with weights given by the probability of having a LoS or NLoS link. In view of the higher altitudes of the drones, we use the model described in [14] for the path loss corresponding to the drone cells, with η_{LoS} and η_{NLoS} path loss components corresponding to LoS and NLoS links, respectively. The probability of having a LoS link is

$$p_{\text{LoS}} = 1 - p_{\text{NLoS}} = \frac{1}{1 + \zeta \exp(-\psi[\arctan(h/d_{\text{2D}}) - \zeta])},$$

with ζ and ψ environmental parameters and h and d_{2D} the height difference and horizontal distance between the user and the drone, respectively.

Besides the path loss and antenna gain, shadow fading also affects the propagation gain. To incorporate this, we determine spatially and site-to-site correlated shadow fading maps for each of the sites according to the model provided in [15], for which we use a site-to-site correlation of 0.5, a decorrelation distance d_{decorr} and a standard deviation $\sigma_{\text{shadowing}}$. Moreover, we impose a minimum coupling loss L_{coupling}.

For the *traffic characteristics*, we assume that users arrive according to a spatially uniform Poisson process with rate $\widehat{\lambda}$ users/s/km^2 (including users in outage) and require a data rate of $R = 0.4$ Mb/s where the mobile device is located at an altitude of 1.5 m. In some examples, we also incorporate the presence of a circular traffic hotspot with radius r_{hotspot}, where we assume that the arrival rate in this hotspot is ρ times higher than elsewhere. For ease of numerical implementation, we will only consider a finite set of possible user locations $u \in \mathcal{U}$ (e.g. pixels in commercial radio network planning tools) where users can initiate a call. For each of these pixels, we assume that users arrive/initiate a call with intensity $\widetilde{\lambda}_u$. This means that for pixels in the hotspot the arrival rate is $\widetilde{\lambda}_u = \rho\widehat{\lambda}$, and pixels outside the hotspot have an arrival rate of $\widetilde{\lambda}_u = \widehat{\lambda}$. We assume the mean call duration to be 2 minutes, i.e., $\beta_{i,k} \equiv \beta = 2$ for all $i \in \mathcal{N}$ and $k \in \mathcal{C}$.

Once a user tries to initiate a call, we first determine which cells provide coverage, if any. To do this we calculate the Reference Signal Received Power (RSRP) in dBm for each cell based on the antenna gain, path loss, shadow fading and transmit powers, and say that a cell provides coverage when the associated RSRP value is at least -120 dBm. In case at least one cell provides coverage to the user, we determine the serving cell as the covering cell with the highest RSRP value. Given this cell selection rule, we define the set $\mathcal{U}_i \subseteq \mathcal{U}$ as all pixels $u \in \mathcal{U}$ that have cell i as serving cell.

For the pixels that are associated with one of the cells, we can now calculate the fraction of resources that a user in this pixel requires using $\omega_u = R/\left((1-\kappa) \cdot B \log_2\left(1 + \text{SINR}_u\right)\right)$. In this formula, SINR_u denotes the Signal-to-Interference-plus-Noise Ratio experienced by pixel u. For the calculation of the SINR, we assume a thermal noise of -106.94 dBm and a noise figure of 8 dB.

B. Derivation of performance evaluation model parameters

To determine the model parameters, we first calculate the total load offered to cell i, which is given by

$$\omega_i^{\text{tot}} = \beta \sum_{u \in \mathcal{U}_i} \widetilde{\lambda}_u \omega_u.$$

We assign pixels to the different classes such that users in pixels of class k require less resources than users in pixels of class $k+1$, but at the same time all classes offer approximately the same amount of load to the serving cell. For this we define

$$\widehat{\omega}_{i,k} = \max\left\{ (\omega_v)_{v \in \mathcal{U}_i} \;\middle|\; \beta \sum_{u \in \mathcal{U}_i} \widetilde{\lambda}_u \omega_u \mathbb{1}_{\{\omega_u \le \omega_v\}} \le \frac{k}{C} \omega_i^{\text{tot}} \right\}$$

as the maximum fraction of resources users of class $k \in \mathcal{C}$ in cell i require, and set $\widehat{\omega}_{i,0} = 0$. Then for $u \in \mathcal{U}_i$ define

$$\mathbb{1}_{i,u,k} = \mathbb{1}_{\{\widehat{\omega}_{i,k-1} < \omega_u \le \widehat{\omega}_{i,k}\}},$$

which evaluates to 1 if a user in pixel u of cell i belongs to class k and 0 otherwise. Using this we can express the arrival rate of class-k users at cell i as

$$\lambda_{i,k} = \sum_{u \in \mathcal{U}_i} \widetilde{\lambda}_u \mathbb{1}_{i,u,k}$$

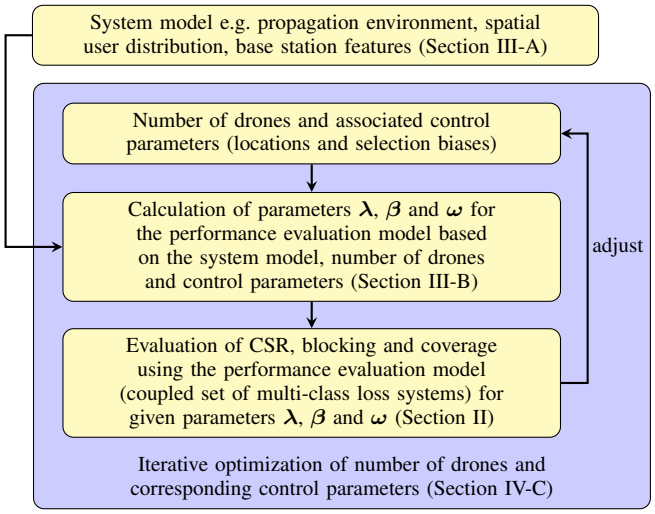

Figure 1: Illustration of the model aspects and their relation.

and the average fraction of resources that class-k users at cell i require as

$$\omega_{i,k} = \frac{\sum_{u \in \mathcal{U}_i} \widetilde{\lambda}_u \omega_u \mathbb{1}_{i,u,k}}{\lambda_{i,k}}.$$

Note that the class structure provides a discretization of the resource requirements ω_u. Therefore, having more user classes increases the granularity and thus the accuracy of the model, but it also increases the computational complexity.

To briefly recapitulate, Figure 1 shows how the different aspects of the model come together and in which section each aspect is described.

IV. Experimental validation

In this section we first describe a set of illustrative scenarios in which the deployment of drone base stations can be useful. Using these scenarios, we determine the number of classes C that the multi-class loss systems of the proposed performance evaluation model require to give accurate results. Furthermore, we show how the performance evaluation model can be used in an iterative optimization to determine the required number of drones and corresponding control parameters to achieve a given target performance level.

A. Scenarios

Recall that our method serves to determine an effective deployment of drone-mounted base stations with the goal to resolve capacity and/or coverage problems. Examples of scenarios for which this method can be used include network disruption events (think of a disaster like a flooding or an earthquake) which results in one or more site failures but also events with massive crowds like festivals or large-scale demonstrations. The decisions that a network operator needs to make are how many drones to deploy, and how to choose their locations and cell selection biases.

To illustrate the use of the proposed method, we will consider a set of ten scenarios. To label these scenarios, we will use the following notation, DU and RU for a dense urban and rural setting, respectively, followed by the number of failing sites and an H if a hotspot is present. With this notation, we consider the following set of scenarios: DU-0-H, DU-1, DU-1-H, DU-2, DU-2-H, RU-0-H, RU-1, RU-1-H, RU-2 and RU-2-H. For these scenarios we consider the parameter values provided in Table I. These values are based on [13], [14], [16], [17]. Furthermore for the dense urban setting, we set the arrival intensity $\widehat{\lambda}$ such that the CSR values are above 98% in normal situations (when all regular base stations work normally, no hotspot has emerged and no drones are deployed). Since coverage should not be a problem in the dense urban setting, the CSR will mainly be determined by the fraction of blocked users. For the rural setting even under normal circumstances few coverage holes may exist, which in general implies that capacity plays a less significant role. Therefore we have chosen the arrival intensity for the rural setting such that approximately 0.1% is blocked in normal situations. However, when a site failure occurs not only the fraction of users without coverage increases, also the fraction of blocked calls increases. The reason for this is that the still operational sites will start to serve part of the area previously served by a failing site, which leads to an increased load of these sites and thus an increased fraction of blocked users.

Table I: Scenario parameters.

Parameter	Dense urban	Rural	Unit
ISD	500	3500	m
h_{antenna}	25	35	m
$\widehat{\lambda}$	1.2	0.014	users/s/km^2
θ_{tilt}	7	4	$^\circ$
ζ	12.08	2.23	
ψ	0.11	0.83	
η_{LoS}	1.7	0.1	dB
η_{NLoS}	24	22	dB
d_{decorr}	45	80	m
$\sigma_{\text{shadowing}}$	5	6	dB
L_{coupling}	70	80	dB
r_{hotspot}	100	300	m
ρ	4	20	

In all scenarios we will only consider different values for the x and y coordinates of the drones. We assume the altitude of the drones to be fixed at 120 m, and do not consider any cell selection biases, or any other optimization parameters like the beam width of the drone antennas. Furthermore, for the calculation of the CSR, we consider a subset of the most impacted regular cells including the cells of the failing sites (if any) and their neighboring cells as well as the drone cells.

B. Impact of C on performance evaluation model accuracy

To determine the number of classes that the model requires to provide sufficiently accurate results, we need to compare the CSR provided by the proposed model to a baseline. For this baseline, we use simulations based on the same modeling assumptions, except that the user locations are continuous instead of the pixels used in the proposed model. Furthermore,

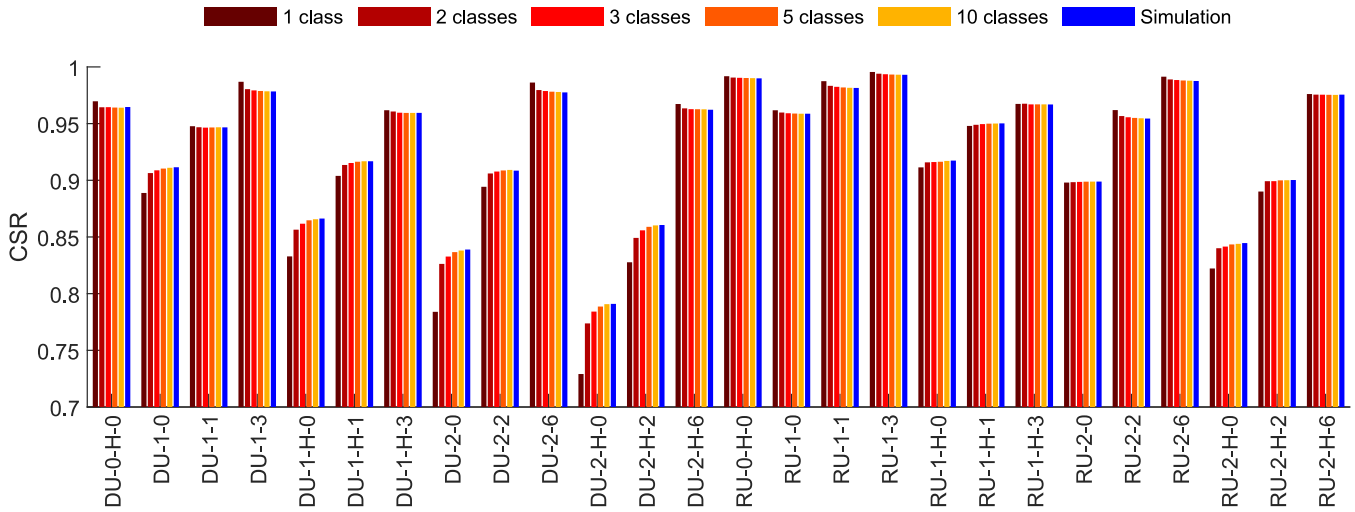

Figure 2: CSR values of theoretical model for different number of classes, and simulation results for various scenarios, where the last number represents the number of deployed drones.

we do not categorize users in classes but account for their actual required fraction of resources.

For the comparison of the CSR values of the proposed model and the simulations, we compare the scenarios described in the previous section and consider no drone deployment when there is no failing site, the deployment of 0, 1 or 3 drones in case of a single failing site and 0, 2, or 6 drones in case of two failing sites. When the number of drones is equal to the number of failing sites (1 or 2), the drones are positioned right above the failing site. For the deployment of 3 or 6 drones, we roughly position these drones above the center of the failed cells (165 m and 1165 m from the failing sites along the azimuth directions for the dense urban and rural setting, respectively). Note that these drone locations are only chosen to compare the CSR of our model to the CSR values obtained from simulations.

Figure 2 shows the CSR values for 1, 2, 3, 5 and 10 classes for the various scenarios. In order to assess the accuracy of the results, we have also added the average CSR of 100 runs of the simulations (the baseline), where the CSR of a single run is measured over a time period of four hours. As we can see, for three or more classes, the CSR of our method is close to the simulated values. To be more precise, using three classes the relative error is less than 1% for all scenarios, and less than 0.5% for 22 out of 26 scenarios. In conclusion, the proposed model requires only three classes to give accurate results, hence we use this to determine the optimal number of drones and their positions in an iterative manner.

C. Optimal drone deployments

As mentioned before, in an emergency scenario it is useful to know how many drones need to be deployed to restore the CSR to a desired level, and what the corresponding set of control parameters of the drones should be. To determine these, we use an iterative procedure that calculates the CSR (using the performance evaluation model) for different sets of control parameters and selects new sets of control parameters based on the CSR values obtained in the previous iteration. For these new sets of control parameters, we consider the set of control parameter that has the highest CSR so far, and select sets of control parameters that are the same except for one parameter that is slightly different.

So given the number of available drones, we can use this optimization procedure to determine the optimal set of control parameters in a given scenario. Let us consider the scenarios listed in Section IV-A with various numbers of deployed drones. Table II presents the theoretical CSR (using three classes) for the best-found set of control parameters for these scenarios. This table shows that in most cases we need at least three drones for each failing site to restore the CSR to the level before the site failures. However, suppose that the goal is to restore the CSR to a target value of 98%, then for the rural setting with a single failing site, the deployment of one or two drones achieves this goal.

Moreover, we observe a decreasing performance benefit from additionally deployed drones. Although not addressed in this paper, in general we note that the deployment of additional drones may also require careful tuning of their altitudes and cell selection biases in order to optimize the performance gains and avoid excessive interference.

Let us now also show the optimal locations found for the various numbers of drones in case of a site failure for the dense urban setting without and with a hotspot in Figures 3a and 3b, respectively. In these figures, the colored dots indicate the best-found locations of the drones, where the different colors correspond to the number of drones that are deployed. The gray shaded areas indicate the best server areas of the network before the site failure, the black triangles mark the location of the failing site and the black circle in Figure 3b indicates the hotspot area.

These figures show that it is not trivial to find the optimal drone locations. For example, for a single drone in the “DU-1”

Table II: CSR for best-found locations for a given number of drones.

Scenario	No failing site	No drone	1 drone	2 drones	3 drones	4 drones	5 drones	6 drones	7 drones	8 drones
DU-0-H	0.9645	0.9645	0.9733	0.9764	0.9788	0.9800	0.9805	0.9822	N/A	N/A
DU-1	0.9830	0.9088	0.9483	0.9661	0.9808	0.9846	0.9870	0.9885	N/A	N/A
DU-1-H	0.9645	0.8617	0.9233	0.9505	0.9715	0.9771	0.9821	0.9855	N/A	N/A
DU-2	0.9830	0.8327	0.8817	0.9172	0.9417	0.9560	0.9690	0.9810	0.9846	0.9868
DU-2-H	0.9666	0.7842	0.8672	0.9045	0.9338	0.9500	0.9639	0.9745	0.9809	0.9841
RU-0-H	0.9904	0.9904	0.9975	0.9977	0.9979	0.9980	0.9981	0.9984	N/A	N/A
RU-1	0.9983	0.9591	0.9825	0.9895	0.9947	0.9961	0.9971	0.9976	N/A	N/A
RU-1-H	0.9904	0.9161	0.9756	0.9884	0.9930	0.9959	0.9969	0.9976	N/A	N/A
RU-2	0.9983	0.8986	0.9352	0.9598	0.9728	0.9797	0.9857	0.9910	0.9928	0.9945
RU-2-H	0.9820	0.8415	0.9337	0.9544	0.9734	0.9799	0.9859	0.9910	0.9932	0.9942

scenario it might seem logical to position the drone right above the failing site, which however turns out to be sub-optimal due to the shadow fading.

Moreover, in the scenario without a hotspot we see that the optimal drone locations are somewhat evenly spread around the failing site. On the other hand, in the presence of a hotspot, the drone locations are more concentrated around the hotspot as more users are located there.

V. Concluding Remarks

In this paper we have proposed a method to determine the blocking and coverage probabilities as well as the CSR of drone-assisted cellular networks. We demonstrated that this method can be used to determine the required number of drones and associated control parameters to restore/improve the CSR to a desired level. As a result, the found optimal number of drones and their control parameters can serve as a good initial configuration for drone deployment in case of crowded events or emergency scenarios. In future research we plan to extend the dynamic adjustment algorithms proposed in [2] for a single drone to a setting with multiple drones.

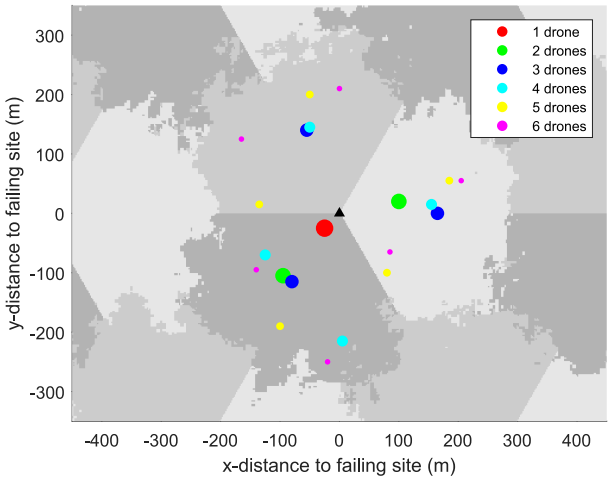

(a) DU-1

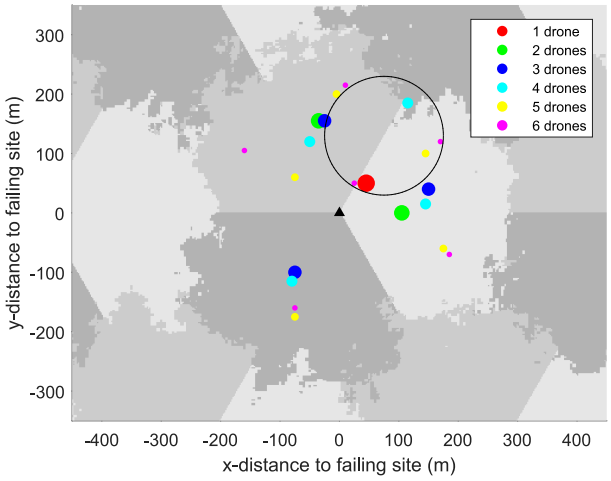

(b) DU-1-H

Figure 3: Best-found drone positions for example scenarios DU-1 (top) and DU-1-H (bottom).

References

[1] 5G!Drones, EU H2020 project, www.5gdrones.eu, 2019-2022.

[2] T.R. Pijnappel, J.L. van den Berg, S.C. Borst and R. Litjens, "Data-driven optimization of drone-assisted cellular networks", *2021 17th International Conference on Wireless and Mobile Computing, Networking and Communications (WiMob)*, 2021.

[3] M. Mozaffari, A. Taleb Zadeh Kasgari, W. Saad, M. Bennis and M. Debbah, "Beyond 5G with UAVs: foundations of a 3D wireless cellular network", in *IEEE Transactions on Wireless Communications*, vol. 18, no. 1, 2019.

[4] F. Al-Turjman, J.P. Lemayian, S. Alturjman and L. Mostarda, "Enhanced deployment strategy for the 5G drone-BS using artificial intelligence", in *IEEE Access*, vol. 7, 2019.

[5] A. Fotouhi, M. Ding and M. Hassan, "Flying drone base stations for macro hotspots", in *IEEE Access*, vol. 6, 2018.

[6] T. Akram, M. Awais, R. Naqvi, A. Ahmed and M. Naeem, "Multicriteria UAV base stations placement for disaster management", in *IEEE Systems Journal*, vol. 14, no. 3, 2020.

[7] E. Kalantari, H. Yanikomeroglu and A. Yongacoglu, "On the number and 3D placement of drone base stations in wireless cellular networks", *2016 IEEE VTC-Fall*, Montreal, Canada, 2016.

[8] X. Wen, Y. Ruan, Y. Li, H. Xia, R. Zhang, C. Wang, W.Liu and X. Jiang, "Improved genetic algorithm based 3-D deployment of UAVs", in *Journal of Communications and Networks*, vol. 24, no. 2, 2022.

[9] J. Li, D. Lu, G. Zhang, J. Tian and Y. Pang, "Post-Disaster Unmanned Aerial Vehicle Base Station Deployment Method Based on Artificial Bee Colony Algorithm", in *IEEE Access*, vol. 7, 2019.

[10] K.W. Ross, "Multiservice Loss Models for Broadband Telecommunication Networks", Springer, 1995.

[11] F. Gunnarsson, M.N. Johansson, A. Furuskär, M. Lundevall, A. Simonsson, C. Tidestav and M. Blomgren, "Downtilted base station antennas - a simulation model proposal and impact on HSPA and LTE performance", *2008 IEEE VTC-Fall*, Calgary, Canada, 2008.

[12] Ericsson. "Ericsson Antenna System Catalog 2021", 2021, pp 487-494.

[13] 3GPP TR38.901: "Study on channel model for frequencies from 0.5 to 100 GHz", *3GPP Technical Report*, v16.1.0, 2019.

[14] A. Al-Hourani, S. Kandeepan and S. Lardner, "Optimal LAP altitude for maximum coverage", in *IEEE Wireless Communications Letters*, vol. 3, no. 6, 2014.

[15] R. Fraile, J. F. Monserrat, J. Gozálvez and N. Cardona, "Mobile radio bi-dimensional large-scale fading modelling with site-to-site cross-correlation", in *European Transactions on Telecommunications*, vol. 19, 2008.

[16] 3GPP TR36.942: "Evolved universal terrestrial radio access (E-UTRA); radio frequency (RF) system scenarios", *3GPP Technical Report*, v16.0.0, 2020.

[17] A. Al-Hourani, S. Kandeepan and A. Jamalipour, "Modeling air-to-ground path loss for low altitude platforms in urban environments", *2014 IEEE GLOBECOM*, Austin, USA, 2014.